Progress In Electromagnetics Research Letters, Vol. 19, 127–135, 2010

NUMERICAL TOTAL SCATTERING CROSS SECTION FROM REVERBERATING ELECTROMAGNETIC EXPERIMENTS

I. El Baba, S. Lalléchère, and P. Bonnet †

Clermont University/Blaise Pascal University
BP 10448, F-63000, Clermont-Ferrand, France

Abstract—The total scattering cross section (TSCS) of various targets is computed in this letter from a numerical method in a reverberation chamber (RC). Theoretically TSCS measurements need both a free-space environment (for instance anechoic chamber modeled numerically by absorbing boundary conditions) and various plane waves' stimulations. The method developed allows predicting the TSCS from few simulations in a RC. The foundations and numerical results presented demonstrate the ability of the technique to straightforward compute the TSCS with the finite difference in time domain (FDTD) method. The agreement from these TSCS treatments in RC is finally obtained considering the expected results in free-space.

1. INTRODUCTION

The mode stirred reverberation chamber (MSRC) has become more and more popular since the last fifteen years, mainly for electromagnetic compatibility (EMC) testing [1]. This is due to their capacity to generate high-peak electric (E-) fields for weak costs and to provide a statistically uniform electromagnetic field within a relatively large domain (called working volume). Under specific conditions, a system placed in the working volume of the MSRC is irradiated by an infinite number of plane waves of random polarization and incidence [2, 3]. Relying on their inner electromagnetic field properties, the device tested in MSRC is embedded in a diffuse electromagnetic environment and standards assessed the use of statistical moments [4]. Far from only EMC applications, many electromagnetic treatments

Received 22 October 2010, Accepted 1 December 2010, Scheduled 8 December 2010
Corresponding author: Ibrahim El Baba (ibrahim.elbaba@lasmea.univ-bpclermont.fr).
† All are also with CNRS — UMR6602/LASMEA, F-63173, Aubière, France.

may need to gather simplicity of MSRC test processes with an accurate idea of incidence and polarization of fields. In this context, different methods and tools have been extensively used to compute the total scattering cross section (TSCS) of various objects [5]. Historically, related to the definition of the radar cross section (RCS), these measurements (experimental and/or numerical) were led in free-space for an object located in the far-field area (relatively to the frequency of the illuminating wave) [6]. In this letter, we adapt and extend an alternative methodology [7] which uses a reverberation chamber (RC) to compute the TSCS of various objects. We put the focus on the numerical setup (RC modeling: losses, sources, probes, targets and post-treatment) needed to compute the TSCS. The validity and an illustration of the method are finally given by comparing results from traditional calculation of TSCS in free-space simulations with ones obtained from simulations in reverberating environment.

2. THEORETICAL PRINCIPLES

The diffuseness of the E-field in MSRC is due to the multiple scattering of waves over the metallic walls of the cavity. High-quality factor (Q) is needed to provide a sufficient number of reflections; obviously the scattering strength of the tested equipment will induce different interactions between object and inner electromagnetic environment. According to [8], Q-factor (losses) may be derived from the sum of various components mainly related to absorbers Q_a and other sources of losses Q_o (walls, antennas, scatterers). If the absorbing cross section (ACS) may be derived from Q_a measurements [9], the computation of the TSCS from simulated RC E-fields may appear particularly important. A double interest exists to compute ACS and TSCS in MSRC. On one hand it enables to quantify Q-factor (ACS) and on the other hand the TSCS of the tested object provides useful data concerning its ability to interact or not with the inner MSRC environment. Over the last decade, numerous MSRC works aimed to characterize accurately the stirrer design (shape and location) [10] according to EMC standard tests [4]. In this letter, the computation is obtained from time simulations involving a pulse source and statistical properties of RC [2]. In the following, without loss of generality the outputs and results are computed for a two-dimensional (2-D) study.

From [6], for a scattering object and a 2-D incident plane wave of a given frequency, polarization, and direction (θ,ϕ), the scattering cross section (SCS (m)) may be written from the scattered (at a far-field distance R (m)) E_s and incident E_i E-fields (V/m) as

$$SCS(\theta,\phi) = 2\pi R \left|E_s\right|^2 / \left|E_i\right|^2 \tag{1}$$

The studied object needs to be illuminated by a large set of plane waves (incidences and polarizations) to completely compute the TSCS (SCS averaged over all directions and polarizations).

Relying on previous remarks, the properties of inner E-fields in RC predict their great interest for TSCS measurements. Actually, a process has been experimentally designed to achieve TSCS measurements in RC combining results from various locations of the sources, measurements probes and object locations [7]. From E-field $E_z(t)$ (2-D TM mode) at time t, we can write a relation involving the mean values respectively over the sources α and probes β (given by $\langle . \rangle_{\alpha,\beta}$) as follows [7]:

$$\left\langle E_z^2(t) \right\rangle_{\alpha,\beta} = \left\langle E_z^2(0) \right\rangle_{\alpha,\beta} \exp\left[-2\pi f t/Q\right] \tag{2}$$

With f the studied frequency (Hz). Given the multi-diffusing environment of MSRC (due to wall, stirrer, tested object), it is necessary to distinguish scattering from various targets. Consequently, previous sets of measurements are achieved several times corresponding to different locations of the studied scatterer. From mean value of E-field over the various object locations δ (denoted by $\langle . \rangle_\delta$), we can write a relation similar to (2) as follows:

$$\left\langle \langle E_z(t) \rangle_\delta^2 \right\rangle_{\alpha,\beta} = \left\langle \langle E_z(0) \rangle_\delta^2 \right\rangle_{\alpha,\beta} \exp\left[-t\left(\frac{1}{\tau_s} + \frac{2\pi f}{Q}\right)\right] \tag{3}$$

The scattering damping time τ_s (s) is directly related to the object TSCS since a relation between TSCS and τ_s is established in [11]; for N objects in an empty (vacuum, celerity c (m/s)) MSRC of area S (m^2), we can write

$$TSCS = S/\left(N\tau_s c\right) \tag{4}$$

In order to compute the TSCS from RC numerical experiments, we define the ratio C as follows:

$$C(t) = \left\langle \langle E_z(t) \rangle_\delta^2 \right\rangle_{\alpha,\beta} / \left\langle E_z^2(t) \right\rangle_{\alpha,\beta,\delta} \tag{5}$$

Indeed, at time $t = 0$, field has not reached the studied object, thus we may deduce that $\langle \langle E_z(0) \rangle_\delta^2 \rangle_{\alpha,\beta} = \langle E_z^2(0) \rangle_{\alpha,\beta,\delta}$. Finally, if the acquiring is sufficient, the part of the field that has been diffracted by the object is not the same in each object position so their average equals to zero, and the field $\langle \langle E_z(t) \rangle_\delta^2 \rangle_{\alpha,\beta}$ decreases faster than $\langle E_z^2(t) \rangle_{\alpha,\beta,\delta}$. Consequently $C(t)$ decrease exponentially and τ_s may be linearly derived from

$$\tau_s(t) = -t/\log\left[C\left(t\right)\right] \tag{6}$$

In the following, based upon the relations (4), (5) and (6), it will be possible to compute entirely the TSCS. In the next section, we will put the focus on the importance of the initial numerical setup.

3. NUMERICAL SETUP

Simulations are led following two distinct formalisms based upon relations (1) and (4). On one hand, from (1), the computation of TSCS may be straightforward achieved from finite difference in time domain (FDTD) [12] simulations in free-space. Studied targets are stimulated by a large number of plane waves (400 incidences that correspond to the maximum number allowed by FDTD discretization, 2 polarizations in 2-D) for the TM mode (Fig. 1(a)).

On the other hand, numerical experiments were achieved in a single RC whose area was $S = 3.27 \times 2.71\,\mathrm{m}^2$ (Fig. 1(b)). The

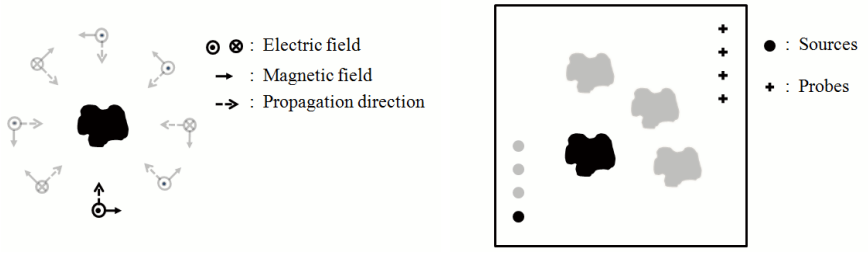

Figure 1. (a) Free-space configuration, with several plane waves aggressing the object under test one by one. (b) Configuration of the TSCS calculation in reverberation chamber. Dark parts correspond to the active configuration in each simulation.

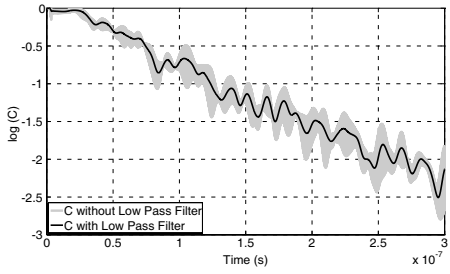

Figure 2. C ratio corresponding to a 10 cm PEC square with and without low pass filter.

numerical RC walls are designed with perfect metallic conductors (PEC) conditions jointly with lossy materials (conductivity s_v) to model Q-factor. A set of 8 points sources representing elementary ideal dipoles were located on a side of the chamber, the distance between two consecutive sources is a half wavelength, whereas the E-field was recorded by 8 probes (elementary ideal sensors) on the other side. The excitation pulse is a gaussian modulated sine pattern with a central frequency $f = 2\,\mathrm{GHz}$ and bandwidth $\Delta\Omega = 100\,\mathrm{MHz}$ at $-6\,\mathrm{dB}$. Simulations are performed with an uniform spatial discretization $dx = dy = 1\,\mathrm{cm} = \lambda/15$ (λ is the wavelength relative to f). Practically, the previous numerical setup is achieved for 30 different positions of the PEC objects introduced inside RC and equally distributed with a distance $d \cong \lambda$ in order to minimize the correlations between acquisitions. The data processing enabled to compute $C(t)$ from (5) by averaging E-fields over the target locations, the sources and electric probes. A low pass filter, applied respectively to the numerator and the denominator of (5), is needed to suppress field fluctuations around $2 \times f$. Fig. 2 shows the variation of $C(t)$ for a 10 cm PEC square target with and without filter.

From (4) and (6), the TSCS may be straightforward deduced considering the linear least-square approximation of the evolution of C with respect with the time t spent in the chamber. A study on the necessary number of sources (S), probe (P) and target positions (M) is shown on Fig. 3, where the $C(t)$ ratio has been plotted for different contributions. In the following (Section 4), we have chosen a set of parameters ($S = P = 8$ and $M = 30$) where the C convergence is clearly reached, thus the robustness of the technique considering various targets can be checked comparing RC and free-space results.

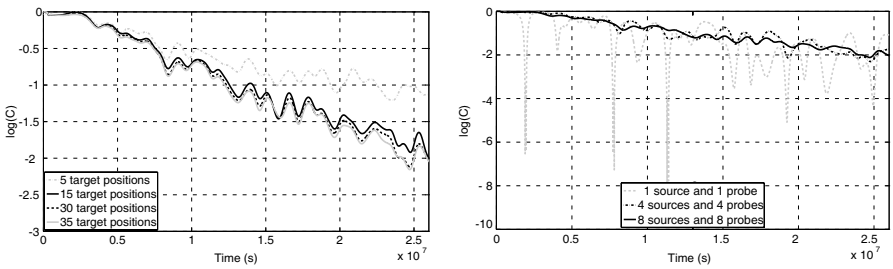

Figure 3. (a) C coefficient corresponding to various numbers of target positions (M) with 8 sources and 8 probes. (b) C corresponding to different number of sources (S) and probes (P) with 30 target positions. The object is a 10 cm PEC square.

4. RESULTS AND DISCUSSION

Although the decay of the E-field is due to the RC load (absorption) and to the target (diffusion), the TSCS appeared relatively independent from RC losses (Fig. 4) as expected respectively theoretically (4–5) and experimentally [7]. On Fig. 4, changing conductivity values ($s_v = 0.01$ or 20 S/m) induced very few variations regarding C. These results were given for a 10 cm PEC square target (Fig. 5(c)). The linear estimation (Fig. 4, black line) appeared common in the post-treatment process. Obviously, the reverberating behavior of E-fields remained crucial to properly compute TSCS. Thus, regarding simulations achieved for an extremely low Q-factor RC (Fig. 4, dashed grey lines: extreme case modeling a pseudo-anechoic chamber), the proposed method may not take advantage from multi-path scattering of RC and may appear inopportune.

We presented on Fig. 6 the TSCS computations from two different formalisms with respect to the Ka criteria (with $K = 2\pi/\lambda$, and a the

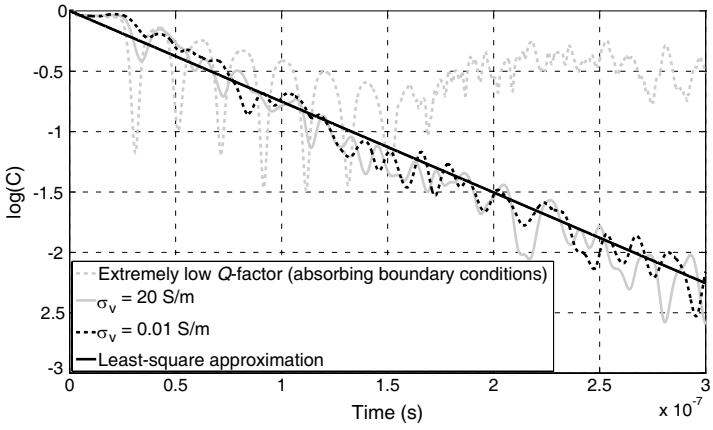

Figure 4. Influence of losses on the ratio C with respect to the simulation time t (linearly related to the damping time τ_s).

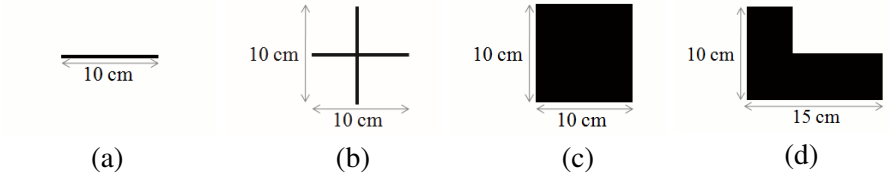

Figure 5. Variety of targets used to compute the TSCS from RC simulations.

side of the studied target). In a first time, the TSCS was deduced from (1) illuminating the target in free-space with a large number of plane waves (incidences uniformly distributed around the object). From a computing cost point of view, free-space modeling requires one FDTD simulation for each plane wave direction and polarization. In a second time, the computation involved formalism developed in this article for RC measurements. Simulations were performed on the same computer (Processor Intel Xeon 2.80 GHz, 3 GB RAM), a 65% time save is obtained from RC simulations comparing to free-space ones. Two different objects were tested (Fig. 6): a PEC square (black) and a PEC wire (grey). The comparison between RC (circle markers) and free-space (full lines) on Fig. 6 showed a great agreement considering different target sizes and shapes. Due to the sizes of the enclosed RC, the tested targets are size-limited but, a priori, no restrictions may be expected from the shape of the object.

Following the same process as depicted previously, the Fig. 7 shows how this technique may reveal useful to distinguish objects. Actually, the least-square approximation of C coefficient for four different targets (Fig. 5) is presented. We may notice that the computed TSCS levels are (0.12, 0.16, 0.22, 0.25 m) respectively for targets ((a), (b), (c), (d)) of Fig. 5. Obviously, the presence of each target implies a typical impact (no influence of course without object, dashed grey line on Fig. 7). According to Fig. 7, the computation of the C coefficient appears sufficiently efficient to properly distinguish objects. Finally,

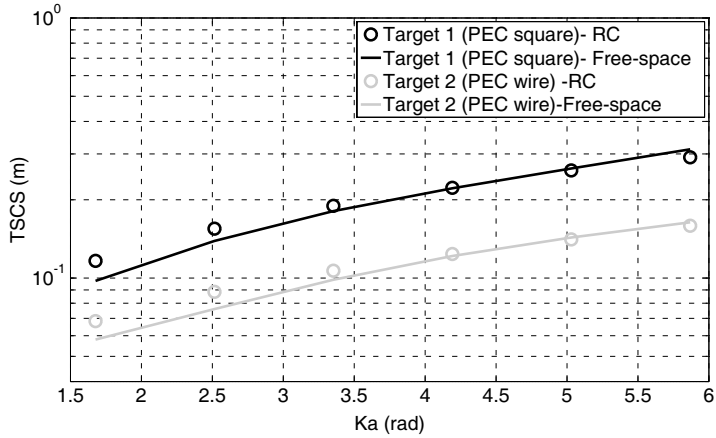

Figure 6. Total scattering cross sections TSCS from reverberation chambers (RC) and free-space simulations for various targets (sizes $a = [4; 6; 8; 10; 12; 14]$ cm).

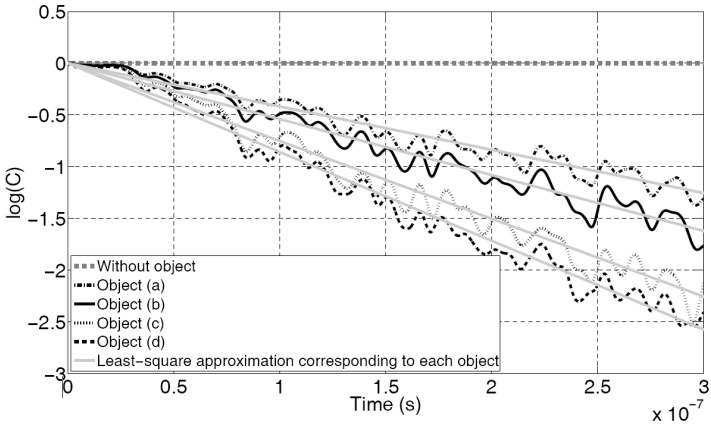

Figure 7. C and its least-square approximation corresponding to the different objects of Fig. 5.

this RC technique provides information about the scattering behavior of targets with weaker computing costs than free-space simulations (especially for three-dimensional (3-D) study, where calculating TSCS in free-space requires a huge number of plane waves' stimulations).

5. CONCLUSION

Measurements of the TSCS in anechoic chambers may appear time consuming and complex. Actually, simulating this problem may reveal the same issues concerning the number of plane waves necessary to properly stimulate the target. In this article, we demonstrate the ability of an original technique to compute the TSCS straightforward from various arrangements of E-field simulations in MSRC. Although only 2-D results were presented, without any loss of generality, same conclusions may be written for 3-D tests. We demonstrate that this technique may bring saves both in time and memory computing comparing to free-space simulations in 2-D. Considering the huger number of plane waves' stimulations needed for free-space 3-D TSCS, this RC method appears all the more efficient. Overstepping the general interest of defining with weaker time costs the TSCS of various targets, a crucial prospect may be expected in MSRC developments considering the importance of the stirrer. Jointly with EMC standards defining the stirrer efficiency, applying this technique to the RC stirrer may bring crucial information to characterize the stirring quality.

REFERENCES

1. Corona, P., J. Ladbury, and G. Latmiral, "Reverberation-chamber research — then and now: A review of early works and comparison with current understanding," *IEEE Trans. Electromagn. Compat.*, Vol. 44, 87–94, 2002.
2. Hill, D. A., "Plane wave integral representation for fields in reverberation chambers," *IEEE Trans. Electromagn. Compat.*, Vol. 40, No. 3, 209–217, 1998.
3. Moglie, F. and A. P. Pastore, "FDTD analysis of plane waves superposition to simulate susceptibility tests in reverberation chambers," *IEEE Trans. Electromagn. Compat.*, Vol. 48, No. 1, 195–202, 2006.
4. "Reverberation chamber test method," *IEC Draft 61000-4-21 Electromagnetic Compatibility (EMC)*, Part 4, Section 21, 2000.
5. Alexopoulos, A., "Scattering cross section of a meta-sphere," *Progress In Electromagnetics Research Letters*, Vol. 9, 85–91, 2009.
6. Beste, J. M., *Reflectivity Measurements, Microwave Antenna Measurements*, 3rd edition, J. S. Hollis, T. J. Lyon, and L. Clayton (eds.), Ch. 13, MI Technologies, Suwannee, GA, 2007.
7. Lerosey, G. and J. de Rosny, "Scattering cross section measurement in reverberation chamber," *IEEE Trans. Electromagn. Compat.*, Vol. 49, No. 2, 280–284, 2007.
8. Arnaut, L. R., "Statistic of the quality factor of a rectangular reverberation chamber," *IEEE Trans. Electromagn. Compat.*, Vol. 45, No. 1, 61–76, 2003.
9. Carlberg, U., P.-S. Kildal, A. Wolfgang, O. Sotoudeh, and U. Orlenius, "Calculated and measured absorption cross section of lossy objects in reverberation chamber," *IEEE Trans. Electromagn. Compat.*, Vol. 46, No. 2, 146–154, 2004.
10. Hong, J. I. and C. S. Huh, "Optimization of stirrer with various parameters in reverberation chamber," *Progress In Electromagnetics Research*, Vol. 104, 15–30, 2010.
11. Ishimaru, A., *Wave Propagation and Scattering in Random Media*, Ch. 14, 253–294, Academic, New York, Vol. 2, 1978.
12. Yee, K. S., "Numerical solution of initial boundary value problems involving Maxwell's equations in isotropic media," *IEEE Trans. Ant. Propagat.*, Vol. 14, 302–307, 1966.